

## Soft X-ray and Low Energy Electron Induced Damage to DNA under N<sub>2</sub> and O<sub>2</sub> Atmospheres

Elahe Alizadeh<sup>1,\*</sup>, Pierre Cloutier<sup>1</sup>, Darel Hunting<sup>1</sup>, and Léon Sanche<sup>1,2</sup>

<sup>1</sup>Département de Médecine Nucléaire et Radiobiologie, Faculté de médecine et des sciences de la santé, Université de Sherbrooke, J1H 5N4, Sherbrooke, QC, Canada

<sup>2</sup>Department of Physics and Astronomy, The Open University, Walton Hall, MK7 6AA, Milton Keynes, UK

### Abstract

DNA damage induced by low energy electrons (LEEs) and soft X-rays is measured under dry nitrogen and oxygen at atmospheric pressure and temperature. Five-monolayer plasmid DNA films deposited on tantalum and glass substrates are exposed to Al K<sub>α</sub> X-rays of 1.5 keV in the two different environments. From the damage yields for DNA, G-values are extracted for X-rays and LEEs. The G values for LEEs are 3.5 and 3.4 higher than those for X-ray photons under N<sub>2</sub> and O<sub>2</sub> atmospheres, respectively. Since most of the measured damage is in the form of single strand breaks (SSB), this result indicates a much higher effectiveness for LEEs relative to X-rays in causing SSB in both environments. The results indicate that the oxygen fixation mechanism, which is highly effective in increasing radiobiological effectiveness, under aerobic conditions, is operative on the type of damage created at the early stage of DNA radiolysis by LEEs.

### Keywords

Radiation damage; Strand breaks; G-values; Oxygen fixation

## 1. Introduction

It is usually accepted<sup>1,2,3,4,5,6,7</sup> that the detrimental biological effects of ionizing radiation, such as X- and  $\gamma$ -rays, are largely caused by damage to the DNA of living cells. This damage is classified as direct and indirect. About half of the DNA damage arises from the direct effect, i.e., from radiation energy deposited directly in the DNA molecule which results in ionization and / or excitation of individual components of the molecule.<sup>8</sup> The indirect effect damage, which has been reviewed extensively,<sup>1,9,10</sup> concerns the interaction of radiation with the local molecular environment surrounding DNA, i.e., water, salts, proteins and oxygen molecules. These interactions result in the immediate formation of

\*Corresponding Author: Elahe.Alizadeh@USherbrooke.ca, Phone number: +1 819 346 1110 (15863), Fax number: +1 819 564 5442.

Supporting Information Available: G values for Al K<sub>α</sub> X-rays of 1.5 keV and low energy electrons (LEEs) are calculated from the yields obtained from the slopes of a linear-least-squares fits of respective exposure curves (Figures 3a and 3b). It is commonly given in SI units as the number of moles of product per Joule of radiation energy present in each primary particles (commonly expressed as  $\mu\text{mol/J}$  or  $\text{nmol/J}$ ). This material is available free of charge via the internet at <http://pubs.acs.org>.

hydroxyl radicals ( $\text{OH}^\bullet$ ) by the radiolysis of water and solvated electrons, both of which react with DNA.<sup>11,12</sup> In either the direct or indirect effect, ionizing radiation generates very large quantities of non-thermal secondary electrons (SEs) in cells ( $\sim 4 \times 10^4$  by a 1 MeV particle) with a most probable energy lying below 10 eV.<sup>13,14</sup> Thus, in recent years much research interest has been focused on the fragmentation and modification of DNA by low energy electrons (LEEs).<sup>15,16,17</sup> In experiments, molecular solid films of DNA held under ultra high vacuum (UHV) were bombarded with LEEs. Below about 15 eV, LEEs were found to induce strand breaks in DNA essentially via the formation of transient anions located on specific DNA components. These transient states can decay by dissociative electron attachment (DEA) or emit the additional electron, leaving the molecular site unaltered or in an electronically excited states.<sup>15</sup> However, it is now well established that the processes induced by electron impact on the bio-molecules are highly dependent on their environment.<sup>16,18,19</sup> To gain further knowledge of LEE-DNA interactions in biological systems, it is therefore important to perform LEE-DNA experiments under conditions closer to those in the cell.

The biological effects of ionizing radiation are known to be significantly affected and modified by the presence of vital cellular components, particularly  $\text{H}_2\text{O}$ ,  $\text{O}_2$  and the histone proteins, which are in contact with DNA.<sup>1,12</sup> Studies dealing with the influence of oxygen on radiation effects in living cells began as early as one hundred years ago and have continued extensively, as one of the most significant subjects in radiation science.<sup>20,21</sup> Quantitative studies of the relationship between oxygen concentration and radiation response has shown that exposure to high concentrations of oxygen causes greater damage in experimental animals and humans and that damage to DNA in malignant cells depends on the oxygenation of the tumor cells; e.g. in the killing of *Escherichia coli* by X-ray radiation at a constant radiation dose.<sup>22,23</sup> In cultured mammalian cells, an oxygen enhancement ratio (OER) of approximately 3 is commonly observed when the cells are irradiated with high doses of X-rays.<sup>24</sup> In other words, the dose required to inactivate a given cell population to a certain level in the absence of oxygen (in a nitrogen atmosphere) can be three times higher than in its presence.<sup>25</sup> In these studies, the presence of oxygen is necessary during the radiation exposure or within a few milliseconds after exposure. The toxic effects of excessive exposure to oxygen were interpreted as due to an increased production of oxygen radicals or other reactive metabolites derived from DNA and oxygen.<sup>26,27,28</sup> More precisely, short-lived free radicals ( $\text{DNA}^\bullet$ ) created by radiation in DNA, react with available  $\text{O}_2$  to generate peroxy radicals ( $\text{DNA-OO}^\bullet$ ).<sup>29</sup> This chemical modification of DNA is more difficult for the cell to repair. The mechanism is generally referred to as the oxygen fixation hypothesis (OFH), because it assumes that the addition of  $\text{O}_2$  to the target radical fixes the damage so that it can not be repaired or restored.<sup>12</sup>

In our laboratory, Cai et al.<sup>30</sup> studied the damage to DNA in vacuum resulting from the emission of low energy secondary electrons from a metal surface exposed to soft X-rays. This method has recently been exploited by Brun et al.<sup>31</sup> to investigate DNA damage under ambient atmospheric conditions. The experiments were performed with DNA films deposited on an insulator (glass substrate) and also on an electron-emitting gold surface under vacuum and atmospheric condition. The G values (i.e., damage per energy absorbed)

for total LEE-induced damage in DNA were measured and the results obtained under the two different conditions compared.

In the present work, the apparatus and the technique developed by Brun et al.<sup>31</sup> has been improved to investigate the LEE damage induced in DNA under well-controlled environmental conditions, at standard atmospheric pressure (STP). Due to the advance in the technique, we are able to isolate DNA films in pure dry nitrogen and oxygen at STP. In our experiments, damage to plasmid DNA is measured in the form of strand breaks or decrease of the supercoiled plasmid population. Damage produced on a glass substrate is attributed to energy absorption from X-rays, whereas that produced on a metal substrate (tantalum) arises from energy absorption from both the soft X-ray beam and secondary electrons emitted from the tantalum surface. From comparison of results obtained with DNA films deposited on tantalum and glass substrates, we deduced the damage created by LEEs. The present results constitute the first comparison of DNA damage induced by photons (Al  $K_{\alpha}$  X-rays of 1.5 keV) and LEEs (average energy of 5.85 eV) under pure nitrogen and oxygen atmospheres. From these, the G values for the direct and indirect effects of LEEs are derived. Furthermore, comparison between our data and those previously reported<sup>30,31</sup> illustrate modifications introduced by an oxygenated environment on DNA damage.

## 2. Experimental Methods

### 2.1. DNA Preparation and Manipulation

pGEM-3Zf(-) plasmid DNA (3197 base pairs, Promega) was extracted from *Escherichia coli* JM109 and purified with the QIAfilter Plasmid Giga Kit (Qiagen).<sup>32</sup> The DNA pellet was then redissolved in TE buffer (10 mM Tris, 1 mM EDTA) with pH 8 to protect the plasmid DNA from degradation. Prior to use, DNA was cleaned up from TE by applying a home-made microcolumn of Sephadex G-50 resin on a bed of glass beads, which is highly efficient for the removal of small molecules, i.e. salts, from a solution.<sup>33,34</sup> After equilibration and washing with distilled and deionized water (ddH<sub>2</sub>O), the plasmid DNA was eluted by centrifugation. It can be accurately characterized utilizing a Synergy HT-I spectrophotometer that gives the DNA concentration by measuring optical density (absorption) at 260 nm, assuming a molar absorption coefficient of  $5.3 \times 10^7 \text{ L} \cdot \text{mol}^{-1} \cdot \text{cm}^{-1}$  at pH 7.0 for DNA.<sup>35</sup> It is well known that the maximal absorption at 260 nm in double-stranded DNA can be correlated in absorbance units with the concentration of the absorbing species.<sup>36</sup> The DNA purity can additionally be determined by calculating the ratio of optical densities at 260 and 280 nm ( $A_{260} / A_{280}$ ), which shows the amount of proteins linked to the DNA molecules,<sup>37,38</sup> since proteins absorb maximally at 280 nm. A ratio close to 2.0 implies a low concentration of proteins. For the plasmid DNA used in this study, this ratio was  $>1.92$ . DNA samples were diluted with ddH<sub>2</sub>O till  $50 \text{ ng} \cdot \mu\text{L}^{-1}$  concentration. Analysis of these plasmids by agarose gel electrophoresis showed that about 96% of the extracted plasmid was in the supercoiled form and the rest were in the nicked circular form ( $> 3\%$ ) and concatemeric form ( $< 1\%$ ).

For each series of measurements, in order to form a constant thickness of approximately 5 monolayers (5ML) of plasmid film on the substrate, a 10  $\mu\text{L}$  drop of solution, containing 500 ng of purified DNA in nanopure water without any added salts, was deposited on the cleaned

glass and tantalum substrates. Deposited samples were frozen at  $-70^{\circ}\text{C}$  and then lyophilized (or freeze dried) by pumping with a hydrocarbon-free sorption pump under the pressure of 1–3 mTorr for around two hours. Each film of dry DNA had a measured area of  $6.0 \pm 0.2$  mm average diameter. Assuming minimal clustering of the plasmids in the solid and thickness of 2 nm for each ML of plasmid, and from a known density of  $1.71 \text{ g/cm}^3$  for plasmid extracted from *E. coli*,<sup>39</sup> this results in a solid film of 10 nm average thickness on the substrates. The dry samples were transferred to the soft X-ray apparatus for irradiation under different environments.

## 2.2. Experimental Setup

The experiments were performed with a home-made apparatus shown schematically in Figure 1. It is composed of a stainless steel chamber evacuated by a mechanical pump to pressure less than 5 mTorr, and connected to a baratron (A) and an adjustable leak valve (B) joined to a nitrogen gas source. A negative potential of 3.4 kV is applied to a concave aluminum cathode (C) through a high-voltage electrical feedthrough (D). To prevent discharge between the cathode and the chamber walls, the former is fixed in a machineable glass-ceramic (Macor) support (E) which is placed as a cap on a long quartz tube (F).

The construction of the Al  $K_{\alpha}$  X-ray source is based on the original design of Hoshi et al.<sup>40</sup> used in many biological experiments for plant cell irradiation. A plasma discharge with 5.5 mA current is formed between this cathode and an aluminum foil target with  $10.5 \mu\text{m}$  thickness (G). Plasma current can be controlled and stabilized by the nitrogen gas pressure in the main chamber with a leak valve. This valve stabilizes the nitrogen pressure at about 20 mTorr in the main chamber. Aluminum atoms are ionized by electrons incident on the Al thin foil and characteristic  $K_{\alpha}$  X-rays with energy about 1.5 keV are emitted towards the He-filled side enclosed volume (H). X-ray traverse the helium gas and then a thin foil of mylar (I) to enter a small chamber, where the plasmid DNA films deposited on the different substrates have been inserted on six aluminum plates of 44.5 mm diameter (J). These plates are fixed at different positions around a brass rotating disc (K) to allow irradiation of samples directly by X-rays, for different periods of time (i.e., various radiation doses) in presence of specific amounts of gases or vapours introduced by valves (L). The distance of  $1.7 \pm 0.05$  mm between the mylar foil and the surface of the plates is occupied by either dry  $\text{N}_2$  or  $\text{O}_2$  gas, which fills the chamber at 1 atm. the different atmospheres. Lyophilized samples of plasmid DNA are placed very close to the mylar foil to avoid too much photon absorption by the surrounding atmosphere.

In the present experiments, 180 samples were exposed to Al  $K_{\alpha}$  X-rays, in the presence of 100% nitrogen and 100% oxygen without any humidity. To delineate the portion of DNA damage caused by X-rays and that arising from the LEE interactions, plasmid DNA films were deposited on two different types of substrate: an insulator substrate, borosilicate glass (Fisher Scientific) of 1 mm thickness, and an electron-emitting tantalum metal substrate. The latter is a film of  $450 \pm 50$  nm thickness evaporated on a 0.4 mm thickness silicon wafer. In a typical experimental run, 18 samples were deposited on the tantalum and 18 on the glass substrate. For each substrate, three samples were controls, i.e., they were lyophilized, kept under the same atmospheric experimental conditions as the irradiated samples, then

recovered, but were not irradiated by X-rays. The remaining 15 samples, were exposed in groups of three, to X-rays of varying fluence. Furthermore, in order to calculate more precisely in each group the number of incident photons, a small piece of GAFCHROMIC® HD-810 radiochromatic dosimetry film (Advanced Materials Group of International Specialty Products Technologies Inc., Wayne, NJ, USA)<sup>41</sup> was inserted on each plate close to the samples. The photographic film also allowed investigating the uniformity of photon fluence on the plates. It showed that the intensity of incident photons in all position of sample holders (after passing the helium gas and Mylar foil) was entirely uniform.

### 2.3. Agarose Gel Electrophoresis

After irradiation, samples were immediately retrieved from the chamber and each DNA film was dissolved within a few minutes from the tantalum and glass surfaces with 95–98% efficiency. The buffer in the solution was Tris-EDTA: 10 mM/1 mM, pH 7.5 (TE buffer). The different DNA plasmid forms were resolved by a 1% agarose gel electrophoresis run in TAE buffer (40 mM Tris acetate, 1 mM EDTA, pH 8.0) at 10 V.cm<sup>-1</sup> for 7 min and 7.5 V.cm<sup>-1</sup> for 68 min. One  $\mu$ L from each recovered solution containing about 50 ng of DNA were prestained by 3  $\mu$ L of 100 $\times$  SYBR® Green I (Molecular Probes™) for loading in each well. Owing to the strong DNA binding affinity of SYBR Green I, it can be used to stain DNA before electrophoresis (prestaining), as well as after electrophoresis (poststaining).<sup>42</sup> In our case, the samples were incubated with SYBR Green I for at least 15 minutes prior to electrophoresis. The gel itself was stained by 8  $\mu$ L of 10,000 $\times$  concentration SYBR Green I. After electrophoresis, stained gels were scanned with the Typhoon-Trio laser scanner (from GE Healthcare) using blue fluorescence mode at an excitation wavelength of 488 nm and filter type 520 nm-bandpass (520 BP 40). To quantify various DNA forms present in the gel slabs, densitometric analysis was performed using ImageQuant software (Molecular Dynamics).

Because of the weaker binding of SYBR Green I to the supercoiled form of DNA compared to nicked circular and linear configurations, a normalization factor was determined as follows: supercoiled DNA was digested by a nicking enzyme, *EcoR1*, in appropriate buffer at 37 °C during one hour; a procedure that results in complete linearization of plasmid DNA. The normalization factor was calculated from the ratio of the signal from the supercoiled DNA and an equal amount of linearized plasmid DNA. In addition, a calibration lane in the gel was produced by digestion of plasmid with nicking enzymes to allow quantification of single strand breaks (SSBs) and double strand breaks (DSBs) within the irradiated samples. To be able to compare the number of breaks in the samples with the calibration lane, equal amounts of supercoiled and digested plasmid were loaded in the wells of agarose gel and stained as usual. For pGEM-3Zf(-) plasmid, a correction factor of 1.4 was determined after quantification by ImageQuant.

### 2.4. Measurement of the Optical Density of Gafchromic Dosimetry Films

In order to measure the optical density, the HD-810 films were stored in the dark for 48 hours after irradiation at room temperature, and then scanned with a HP ScanJet 4400C color scanner. The output resolution was set at 300 dpi, the output type was set as “true colour”, and the intelligent scanning technology was turned off. The average pixels for blue

and red channels images were read from histogram in ImageJ software.<sup>43</sup> The absorbance was defined as  $\log_{10}(I_0/I)$  where  $I_0$  and  $I$  are the mean values resulting from the ImageJ colour analysis histograms for un-irradiated and irradiated areas of the films, respectively.

Calibration of the sensitivity of the film was obtained by irradiating film samples with X-rays produced by a PHI Model 04-548 Dual Anode X-ray photoelectron spectrometer (XPS, Perkin-Elmer) with an aluminum target. Three pieces of HD-810 films (1.2 cm  $\times$  1.2 cm) were fixed on the stainless steel target holders, irradiated by Al  $K_{\alpha}$  X-ray in an ultra-high vacuum (UHV) chamber for three various periods of time. By the nominal power applied to the anode with the voltage kept constant at 4 kV, nominal power 8 W and with measured emission current of 1.1 mA, the incident fluence rate of photons ( $\Phi_0$ ) was determined to be  $1.14 \times 10^{10}$  photons/s.cm<sup>2</sup>. Then the  $\log_{10}(I_0/I)$  given by Gafchromic films analysis was plotted versus the irradiation time (minutes), and corresponding slope,  $0.0393 \text{ min}^{-1}$ , was used as a factor to convert the irradiation time to photon fluence (photon/cm<sup>2</sup>), in all other experiments.

## 2.5. Calculation of X-ray Attenuation

After emission from the aluminum foil, Al  $K_{\alpha}$  X-rays travel through three different environments before reaching the DNA surface: the He-filled volume of 50 mm thickness, the Mylar foil of thickness 2.5  $\mu\text{m}$ , and finally the atmosphere on top of the film of thickness of about 1.25 mm. Taking the mass attenuation coefficient of helium ( $\mu/\rho = 16.76 \text{ cm}^2/\text{g}$ ) and its density ( $\rho = 8.375 \times 10^{-5} \text{ g/cm}^3$ ), Mylar ( $\mu/\rho = 953.6 \text{ cm}^2/\text{g}$ ) and its density ( $\rho = 1.38 \text{ g/cm}^3$ ), nitrogen ( $\mu/\rho = 1083 \text{ cm}^2/\text{g}$ ) and its density ( $\rho = 1.165 \times 10^{-3} \text{ g/cm}^3$ ), and oxygen ( $\mu/\rho = 1549 \text{ cm}^2/\text{g}$ ) and its density ( $\rho = 1.332 \times 10^{-3} \text{ g/cm}^3$ )<sup>44</sup> and applying the exponential attenuation law  $I_t = I_0 e^{-(\mu/\rho \cdot \rho \cdot x)}$ , the intensities of photons at the DNA surface in  $\text{N}_2$  and  $\text{O}_2$  atmospheres are found to be 60% and 55% of the initial intensity ( $I_0$ ), respectively. Before reaching the surface of the DNA films, 14.7% and 22.9% of soft X-rays are absorbed by  $\text{N}_2$  and  $\text{O}_2$  molecules, respectively.

For X-ray absorption by the plasmid DNA film, we calculated  $\mu/\rho = 1056 \text{ cm}^2/\text{g}$  based on the DNA's composition and  $\mu/\rho$  of individual atoms. Thus, for 5 ML DNA films (10 nm thickness), 0.2 % of soft X-ray photons interact with DNA at the film surface, while 99.8% pass through the film to reach the substrate.

## 2.6. SE Emission from Tantalum

In experiments involving LEE interactions with DNA, tantalum has already been shown to be a suitable substrate. The formation of an oxide layer on the metal surface creates a stable and chemically inert surface, ensuring no direct DNA-metal interaction, thus causing minimal DNA substrate induced damage in the presence of organic ions.<sup>45,46</sup> Lyophilization on other metal substrates can produce considerably more damage; for example, a gold surface induces up to 25% SSB to 5 ML unirradiated buffered DNA films in the vacuum.<sup>31</sup> In our experiments where DNA was lyophilized on tantalum and glass and immediately recovered without exposure to radiation, the induced damage was less than 1%.

X-ray photons that traverse the DNA film interact with atoms in the metal mainly via the photoelectric effect. This interaction causes the emission of energetic photoelectrons and Auger electrons from the metal atoms. These electrons lose energy in the metal and a small portion of them reach the metal surface. The latter produce at the surface a distribution consisting essentially of LEE. The secondary electron energy distribution curve from a tantalum substrate is shown in Figure 2. For fast secondary electrons (SEs,  $E_k > 10$  eV), the relative energy distribution was measured using an analytical X-ray photoelectron spectrometer (XPS, Perkin-Elmer) under UHV conditions; for slow SEs ( $E_k < 10$  eV) it was obtained from Equation 1:<sup>47</sup>

$$\eta(E_k) = \eta_s E_k / (E_k + W)^4 \quad (1)$$

where  $\eta(E_k)$  is the yield of SEs having kinetic energy of  $E_k$ ;  $\eta_s$  is the yield normalization coefficient, and  $W$  the work function of tantalum (i.e.,  $4.3 \pm 0.1$  eV for a vacuum deposited film of tantalum<sup>48</sup> and  $4.22 \pm 0.02$  eV for the bulk substrate of tantalum<sup>49</sup>). The electron energy distribution peaks at 1.4 eV and the average energy is 5.85 eV. The average energy for SEs with energies less than 10 eV is 3.1 eV. From comparison of the area under the curve in two energy regions, we find that more than 95% of electrons emitted from the tantalum have energies less than 30 eV. A total electron yield of 0.049 electrons per photon is obtained from this distribution.

The current of SE emitted from the tantalum surface, induced by incident X-rays in vacuum, was measured to be  $0.17 \pm 0.02$  nA, utilizing a Keithley 610C electrometer connected between the tantalum target ( $1.4 \text{ cm} \times 1.4 \text{ cm}$ ) and the ground. Consequently, the electron flux was calculated to be  $(0.54 \pm 0.2) \times 10^9$  electrons/s.cm<sup>2</sup>. Taking the incident fluence rate of photons ( $\Phi_0 = 1.14 \times 10^{10}$  photons/s.cm<sup>2</sup>) and the total energy-integrated electron yield (i.e., the number of emitted SEs of the different kinetic energies per normally incident photon) we find that  $0.047 \pm 0.005$  electron are emitted per photon. This value is in excellent agreement with 0.04 calculated from the electron current distribution in Figure 3. It is comparable with that of  $0.039 \pm 0.003$  electrons per photon for tantalum, from the work of Cai et. al,<sup>30</sup> and 0.063 electrons per photon for a gold, from work of Brun et. al.<sup>31</sup>

### 3. Results

#### 3.1. DNA Damage as a Function of X-ray and LEE Irradiation

Agarose gel electrophoresis separates different forms of plasmid DNA, including supercoiled (SC), concatemeric (CM), linear (L), nicked circular (C), cross linked form 2 (C-S) and cross-link form 1 (C-C) of DNA. The SC, C and L correspond, respectively, to undamaged DNA and the formation of SSBs and DSBs in the present work, where the loss of supercoiled DNA in both environments and on different substrates happens mostly via formation of circular DNA.

Figure 3(a) shows the dependence of the loss of the supercoiled configuration under X-ray exposure in dry nitrogen, for deposition of the DNA on glass and tantalum substrates. Each

point represents the mean of measurements on three samples, prepared under the same conditions and the error bars represent  $\pm$  standard deviation of the means. Figure 3(b) shows the loss of the supercoiled DNA as a function of photon fluence under an oxygen atmosphere at STP. The loss of supercoiled DNA is fitted as a decreasing linear function of X-ray fluence in both cases.

### 3.2. Damage to Unirradiated DNA Films

Table 1 shows the percentage of undamaged DNA from the solution, as well as the percentage resulting from the damage induced from lyophilization and a three hour exposure to  $N_2$  and  $O_2$  atmospheres. The latter two values were taken from the first point of each curve in Figures 3(a) and 3(b). Damage from lyophilization onto tantalum and glass substrates was obtained by immediate recovery of DNA after deposition. In this case we observe only a negligible increase (less than 2%) in the production of SSB relative to that existing in the 'fresh' DNA solution. For the control samples, which are left on the substrates for periods of three hours, while the other samples are being irradiated, the loss of SC is greater in all cases than when DNA is promptly recovered. Additionally, there appears to be significantly greater damage to these unirradiated samples when they are deposited on tantalum rather than on glass and this, irrespective of the ambient atmosphere; i.e., the percentage of SC recovered from unirradiated samples deposited onto tantalum are smaller by about 7% and 9% in  $N_2$  and  $O_2$ , than the percentage of those deposited onto glass substrates. Also, changing ambient gases from  $N_2$  to  $O_2$  enhances damage to the plasmid, without irradiation. Additionally, as shown in Figure 3(a) and Table 1, for unirradiated DNA films in dry  $N_2$  atmosphere on the glass substrate, samples have almost the same percentage of intact plasmid as the control samples (i.e., the surface causes no SSB). However, the percentage of supercoiled DNA for the tantalum substrate in  $N_2$  atmosphere without radiation is about 88% (corresponding to the loss of 8% of supercoiled DNA), which can be attributed to reactivity of the metal surface. Furthermore, the percentage of supercoiled DNA on the glass substrate in an  $O_2$  atmosphere without irradiation is 91% (or loss of 5% of supercoiled DNA) suggesting that, whereas  $N_2$  induces no damage, oxygen by itself (i.e., without the DNA-metal interaction) degrades the films. Interestingly, these two damages collectively (i.e.,  $8\% + 5\% = 13\%$ ) are almost the same as that observed in unirradiated samples in an  $O_2$  environment for deposited plasmid DNA on tantalum (i.e., about 14%).

### 3.3. Damage to Irradiated DNA Films

The percentage yields per  $10^{12}$  photons. $cm^{-2}$  are obtained from linear fitting of the curves in Figure 3 (a–b) and given in Table 2. The slopes of the fitted lines, which represent the rate of loss of the supercoiled DNA, increase by factors of 1.8 and 1.9, from  $N_2$  atmosphere to  $O_2$  atmosphere for DNA deposited on tantalum and glass, respectively. Furthermore, the enhancement factors (EF) due to LEE interactions which were derived from these values, appear in the last column of the table; they were calculated by dividing the yield obtained with the DNA on the tantalum substrate by that measured with DNA films on the glass. LEE emission from the metal substrate enhances DNA damage by factors 1.4 and 1.3 in the nitrogen and oxygen atmosphere, respectively.



Additionally, the damage yields can be expressed in terms of  $G$  value, i.e., the number of modified molecules or products per unit of energy absorbed by the target. In the current work, the  $G$  values for 1.5 keV soft X-rays and LEEs are calculated in two different units,  $D/100\text{eV}$  and  $\text{nmol/J}$ , where  $D$  represents one damaged DNA molecule. Results are shown in Table 3 and details of the calculation are presented in supporting information.

As shown in Table 3, the  $G$  value for X-rays in an  $\text{N}_2$  environment is  $65 \pm 6 \text{ nmol/J}$  which is less than that in vacuum experiment performed by Cai et al.,<sup>30</sup> i.e.,  $80 \pm 1$  for thick films of DNA. This difference is due to higher film thickness (larger amount of DNA) in the experiment of Cai et al. The  $G$  value for LEEs in  $\text{N}_2$  is  $227 \pm 15 \text{ nmol/J}$ , that is comparable with measurements performed by Cai et al.<sup>30</sup> in vacuum, who found a  $G$ -value of  $277 \pm 42 \text{ nmol/J}$  for a monolayer film. More importantly, our data shows that the ratio of these two  $G$ -values ( $G_{\text{LEE}} / G_{\text{X}}$ ) under nitrogen atmosphere is 3.5 that is exactly the same ratio as in vacuum in the work of Cai et al.<sup>30</sup> Another comparison can be done with results of Brun et al.,<sup>31</sup> i.e.,  $G$ -value of  $400 \pm 200 \text{ nmol/J}$  for LEEs. These results show a similarity between vacuum and  $\text{N}_2$  environments in the study of induced damage on DNA films by soft X-rays and LEEs. In the experiments under an oxygenated atmosphere,  $G$  values are  $124 \pm 9 \text{ nmol/J}$  and  $415 \pm 15 \text{ nmol/J}$  for X-ray and LEEs, respectively, i.e., in an oxygenated atmosphere the  $G$  values are 1.9 and 1.8 times higher than the corresponding value in a nitrogenated environment, for X-ray and LEE, respectively. The  $G$  values for LEEs compared to those of X-ray photons are 3.5 and 3.4 higher under  $\text{N}_2$  and  $\text{O}_2$  atmospheres, respectively. Thus, when the same amount of energy is deposited in DNA by photons or LEEs, the latter are 3.5 and 3.4 times more efficient in causing DNA damage and produce much more strand breaks in the samples. Thus, the enhancements of  $G$  values are essentially independent of the surrounding gases.

The formation of linear DNA (via a DSB) is observed for plasmids deposited on tantalum (and at a much lower level, on glass) but only when irradiated under oxygenated conditions. Under a nitrogen atmosphere, the yield of DSBs, lies below the limit of detection at all photon fluences. Using the energy distribution of secondary electrons from a tantalum substrate (Figure 2), it is possible to plot the SSB and DSB damage yield against the number of secondary electrons to which the DNA was exposed. Figure 4 shows the yield of circular and linear DNA molecules induced by LEEs in an  $\text{O}_2$  environment as a linear function of number of electrons. The ratio of the yields of SSB to DSB is 9:1. This value may seem high compared to previous measurements<sup>45</sup>; however, in our experiment, SSB can be induced by secondary electrons of all energies while only electrons of more than 5 eV are capable of causing a DSB.<sup>5</sup>

#### 4. Discussion

The mechanisms of damage relevant to these results can be considered as belonging to two distinct categories. First, the 'direct' interactions of the Al  $K_{\alpha}$  X-rays and secondary electrons (including LEEs emitted from tantalum substrate) with DNA molecules. The second category, termed 'indirect' interactions includes reactions with DNA of species created by X-rays and secondary electrons in the atmospheres surrounding the DNA (i.e.,  $\text{N}_2$  or  $\text{O}_2$  molecules within the DNA film as well as at the film-gas interface). Mechanisms

operating in first group have been reported and discussed in detail in previous works as a reason for the higher G values observed for damage to DNA by LEEs compared to those of X-rays, in vacuum.<sup>31</sup> In essence, since the interaction of 1.5 keV X-rays with DNA is mainly via the photoelectric effect, photoelectrons and Auger electrons of comparatively high energy are first produced. About 20% of the energy deposited by these fast electrons into cellular material, leads to vibrational and electronic excitation of bio-molecules, whereas the remaining energy leads to ionization and formation of secondary electrons with a wide energy distribution centered around 10 eV.<sup>14,50,51</sup> Whereas X-rays and fast electrons produce electronic and vibrational excitation in a similar proportion, the relative abundance of dissociation states may be larger for LEEs due to the formation of transient anions. Such behavior would result in an additional number of dissociative states and highly reactive radicals and ions produced per unit energy deposited by LEEs. Owing to induced polarisation, it takes less energy to break a chemical bond with a LEE<sup>52</sup> than with a photon.<sup>53</sup> The relatively high yield<sup>52</sup> and cross section<sup>54</sup> to produce a SSB in DNA with LEE, in the 0–5 eV range, indicates that SEs emitted from tantalum could cause considerable damage in DNA via the DEA process, which should result in higher G values for LEEs.

For a discussion of the ‘indirect’ processes, we consider the interaction of Al  $K_{\alpha}$  X-rays with the molecules surrounding DNA. We calculate that 14.7% and 22.9% of soft X-rays are absorbed by  $N_2$  or  $O_2$  molecules, respectively, before reaching to the surface of the DNA films. Therefore, the higher attenuation coefficient of oxygen relative to nitrogen<sup>44</sup> causes greater energy absorbance by  $O_2$  molecules. In the photoelectric process, for such low atomic number elements, almost all of the absorbed photons’ energy is transferred to the kinetic energy of bound electrons<sup>55</sup> and some fast electrons are thus produced in the atmosphere surrounding the DNA film that could interact with other  $N_2$  and  $O_2$  molecules. As already mentioned, about 80% of the X-ray energy deposited in  $N_2$  and  $O_2$  leads to the ionization reactions. A fraction of molecular ions formed may also dissociate via  $h\nu + AB \rightarrow AB^+ + e^- \rightarrow A^+ + B + e^-$ .<sup>11</sup> Ionization potential for these reactions are 15.54 eV for  $N_2^+/N_2$ , 14.53 eV for  $N^+/N_2$ , 12.07 eV for  $O_2^+/O_2$  and 13.62 eV for  $O^+/O_2$ , i.e., less energy is always required for the electron impact ionization of  $O_2$  than that for  $N_2$  molecules.<sup>56</sup> Furthermore, the ionization cross section maxima are  $2.55 \times 10^{-16} \text{ cm}^2$  and  $2.72 \times 10^{-16} \text{ cm}^2$  for  $N_2$  and  $O_2$  molecules, respectively, and the total cross sections for electron impact ionization of  $O_2$  molecules are greater than that for  $N_2$  over the entire photoelectron energy range (10–1000 eV).<sup>57,58</sup> As the energy of incident ionizing electrons increases, various new processes come into play. Additionally, the rest of the absorbed radiation energy produces excited molecules which may dissociate to produce ionized or neutral atoms via reactions  $N_2^* \rightarrow (N^+ + N^-, N + N)$  and  $O_2^* \rightarrow (O^+ + O^-, O + O)$ .<sup>59</sup>

Another process well-described in the literature<sup>59,60</sup> that may occur in the surrounding atmosphere is electron attachment of the low energy SEs produced by the fast electrons. These LEEs arise from transient anions in gas-phase  $N_2$  and  $O_2$ . The incident electrons produce nitrogen atoms and  $O^-$  ions via the following reactions: (1) formation of core-excited anion,  $N_2^{-*}$ , dissociating into  $N(^4S) + N(^3P) \rightarrow N(^4S) + N(^4S) + e^-$ . The dissociation energy for this molecule is  $D(N-N) = 9.76 \text{ eV}$  and the maximum dissociative cross section<sup>61</sup> is  $2.5 \times 10^{-18} \text{ cm}^2$ . Under an  $O_2$  atmosphere, excitation from of Frank-

Condon region of ground state  $O_2$  favours a 6 eV and 8.4 eV process leading to two electronic dissociation channel, one resulting in a ground state  $O(^3P)$ , and another resulting in an excited state  $O(^1D)$ ,  $e^- + O_2 \rightarrow O_2^{-*} \rightarrow O^-(^3P) + O(^3P, ^1D) + e^-$ .<sup>62,63</sup> The dissociation energy,  $D(O-O) = 5.16 \text{ eV}$ <sup>58</sup> is about half of the dissociation energy for  $N_2$ , and the cross section for dissociative attachment of electrons to  $O_2$  metastable molecules<sup>60</sup> is  $4.8 \times 10^{-18} \text{ cm}^2$ . Additionally, in an oxygen atmosphere, a small fraction of LEEs can participate in a three-body attachment reaction to form  $O_2^-$  from  $O_2$  via  $e^- + O_2 + O_2 \rightarrow O_2^- + O_2$ .<sup>64</sup>  $O_2^{\bullet-}$  is known to cause oxidative DNA damage through its combination with guanine neutral radicals.<sup>65</sup> There are some more molecular dissociation and ionization reactions that result in producing various ions and minor neutral species from  $N_2$  and  $O_2$  but we will not consider them here. Furthermore, studies on vibrational excitation of these molecules by electron impact shows excitation of a number of vibrationally excited states for both molecules by LEEs, which are believed to be of little relevance to DNA damage. These excitations have been widely investigated in detail in the literature and are not discussed in this article.<sup>66,67</sup>

A priori, all of the species formed by electron impact can react with DNA. There are a number of reactions that result in the formation of oxygen radicals mentioned in work of Barilla et. al.<sup>18</sup> But the most effective radical is  $HO_2^{\bullet}$  that is preferentially formed via the reaction  $H^{\bullet} + O_2 \rightarrow HO_2^{\bullet}$ . In our case  $H^{\bullet}$  could arise from LEE interaction with DNA. It has been shown that DNA components such as all nucleobases and deoxyribose molecule undergo DEA at sub-excitation energies ( $< 3 \text{ eV}$ ) leading to ejection of a large amount neutral hydrogen radicals.<sup>68,69,70</sup> The  $HO_2^{\bullet}$  radical may be involved in DSB formation,<sup>18</sup> in accordance with the present observation that the formation of the linear form of DNA (via DSBs) is only observed under oxygenated conditions at high photon fluencies (see Figure 4). In contrast, reactive nitrogen species are produced only from the reactions of  $NO^{\bullet}$  and  $O_2^{\bullet-}$ , which are actually require the presence of oxygen species. The production of reactive nitrogen species is related to the presence of  $O_2$  or  $NO_2$  in the environment and nitrogen species always act together with reactive oxygen species to attack DNA.<sup>71,72,73</sup> Therefore, it appears that in pure dry nitrogen (i.e., in the absence of oxygen molecules and its reactive species), much less damage is induced in plasmid DNA films from the indirect effect.

Finally, we must consider that molecules at atmospheric pressure and room temperature have a mean free path shorter than  $0.1 \mu\text{m}$ . Thus, most reactive species formed in the nitrogen or oxygen atmosphere are likely to react with other molecules before reaching to the DNA film. We conservatively estimate that only reactive excited gaseous species formed in a region no more than  $1 \mu\text{m}$  from the surface of the DNA film can interact with the film to cause damage. In this volume, 0.01 % and 0.02 % of the soft X-rays, will be absorbed by  $N_2$  and  $O_2$ , respectively. This is a very small fractions of the total energy deposited but it is still 5% to 10% of the energy absorbed by our 5 ML DNA film. Since twice as much energy is absorbed in  $O_2$  molecules,<sup>44</sup> more reactive species are produced close to the DNA surface, giving a higher probability for oxygen species of reacting with the film. The next important consideration is diffusion within the DNA layers of  $N_2$  and  $O_2$  molecules as well as their relevant reactions species formed after irradiation. The calculation in the appendix of this

article shows that about 52 molecules of  $N_2$  and  $O_2$  diffuse in each plasmid molecule, or one molecule per 124 nucleotides.

Ground state  $N_2$  molecules are not expected to perturb DNA, but here again the situation is different for  $O_2$ . Presently, the most widely accepted explanation for the higher radiation damage to DNA in an oxygenated environment is the oxygen-fixation hypothesis (OFH), which was briefly mentioned in the introduction of this article. Therefore, in our experiments, the short-lived free radicals in DNA arising from the direct interaction of soft X-rays and LEEs, can react with available  $O_2$  molecules in the environment. The reaction can change the chemical composition of DNA to generate an organic peroxide, i.e., peroxy radical ( $DNA-O_2^*$ ), a non-restorable form of the DNA molecule.<sup>12,74</sup> The oxygen is said to 'fix' or make permanent the damages formed by radiation. On the other hand, in the dry nitrogen atmosphere, DNA radicals can be reduced, restoring the DNA to its original composition (DNA-H), and the damaged DNA molecules recover the ability to function normally. Thus, from these arguments and those on the diffusion length of excited nitrogen species in the surrounding gases, it appears that a  $N_2$  atmosphere is not able to increase the damage to the DNA films as evidenced by the similar G-values in vacuum and nitrogen for X-rays as well as for LEEs. On the other hand, under an oxygen atmosphere, the oxygen fixation mechanisms and/or the larger amounts of reactive species produced with their larger reactivity increase the G values by a factor of about two compared to the vacuum value.

Finally, DNA damage by oxyl radicals derived from reactions of the metal substrate must be considered to explain the higher DNA damage for deposited plasmid on the tantalum than glass substrate. Many investigations of the effects of metal ions on DNA cleavage have been conducted. It has been shown that hydrogen peroxide ( $H_2O_2$ ) acts as a much stronger oxidant when decomposed by some metal ions, such as ferrous, nickel (II) and cobalt (II), resulting in DNA damage via the Fenton reaction. The  $H_2O_2$  does not react directly with DNA, but results in the formation of  $HO^*$  in the presence of certain metal ions<sup>75,76</sup> especially those of iron and copper.<sup>77</sup> Thus, damage caused by the metal could be 'fixed' by  $O_2$  which would explain the higher DNA damage in unirradiated films under oxygenated conditions (see Table 1). Also, it should be noted that metals may generate reactive oxygen species from hydroperoxides which arise on DNA sugars and bases and may oxidize these components.<sup>78</sup>

## 5. Conclusions

We have described an improved system to investigate DNA damage induced by soft X-rays (1.5 keV) and LEEs (0–30 eV) under different controllable atmospheres. From the results obtained with DNA films held in pure  $N_2$  and  $O_2$  environments, we determined the G values for DNA strand breaks induced by 1.5 keV photons and LEEs under conditions closer to those of the cell than possible in previous experiments. If it is assumed that the so-called direct effects of radiation in the cell correspond to the damage induced by X-rays in dry DNA under vacuum.<sup>30</sup> The similarity between G values obtained under vacuum and  $N_2$  atmospheres, indicates that gaseous  $N_2$  at STP does not promote radiation damage and hence does not cause an 'indirect' effect of the radiation. In other words, DNA damage induced by the reaction of nitrogen ions and radicals generated around the DNA by photons and LEEs

lies below our detection limit. Changing the atmosphere from N<sub>2</sub> to O<sub>2</sub>, however, while keeping all other experimental parameters constant, increases radiation damage to DNA by factors of 1.9 and 1.8 for X-rays and LEEs, respectively. Thus, the presence of O<sub>2</sub> at STP almost doubles the damage induced by X-rays and LEEs under vacuum. Even though, the ions and radicals produced around DNA in an O<sub>2</sub> atmosphere are about twice as numerous as those produced in an N<sub>2</sub> atmosphere, it appears highly unlikely that this factor alone could explain a 100% increase in DNA damage in O<sub>2</sub> compared to vacuum, while the N<sub>2</sub> environment has no detectable effect within error limits. However, the radicals and ions produced by O<sub>2</sub> are expected to be more reactive than those arising from N<sub>2</sub>. No doubt this higher reactivity could contribute to an increase in damage under the O<sub>2</sub> atmosphere, but probably not cause the huge difference between the two environments. We therefore suggest that the major contribution to the indirect effect of oxygen arises from the reaction of O<sub>2</sub> with already damaged DNA. This reaction would 'fix' the damage or transform radiation-induced non-strand break-type lesions into strand breaks. Thus, the damage created by LEEs at the very early stage of DNA radiolyses in cells could be 'fixed' by oxygen.

When unirradiated DNA films are subjected to the same experimental conditions as the irradiated films under an N<sub>2</sub> atmosphere, the tantalum substrate is found to damage 8% of the original amount, a value which increases to 15% under O<sub>2</sub>. Experiments with DNA deposited on glass in the presence of oxygen indicate that this difference either arises from damage caused by O<sub>2</sub> in the film, or from the transformation into SSB, or fixing, of pre-existing lesions by the presence O<sub>2</sub>. Thus, even in unirradiated films, oxygen fixation could play a role in our experiments. More generally, our results provide evidence for oxygen fixation of the immediate damage to DNA created by secondary electrons within femtosecond times after the primary interaction of high energy radiation in cells.

## Supplementary Material

Refer to Web version on PubMed Central for supplementary material.

## Acknowledgments

The authors gratefully acknowledge the helpful comments and suggestions in this work of Dr. Andrew Bass. Thanks are also extended to Sonia Girouard for the technical support in preparation of plasmid DNA. This research was supported by the Canadian Institutes of Health Research (CIHR) and the Marie Curie international incoming fellowship program.

## References

1. Von Sonntag, C. *The Chemical Basis of Radiation Biology*; Taylor and Francis; London: 1987.
2. Goodhead DT. *Can J Phys*. 1990; 68:872–886.
3. Horan AD, Giandomenico AR, Koch CJ. *Radiat Res*. 1999; 152:144–153. [PubMed: 10409323]
4. Ito T, Baker SC, Stickley CD, Peak JG, Peak MJ. *Int J Radiat Biol*. 1993; 63:289–296. [PubMed: 8095278]
5. Boudaïffa B, Cloutier P, Hunting D, Huels MA, Sanche L. *Science*. 2000; 287:1658–1660. [PubMed: 10698742]
6. Michael D, O'Neill P. *Science*. 2000; 287:1603–1604. [PubMed: 10733428]
7. Spothem-Maurizot, M., Mostafavi, M., Douki, T., Belloni, J. *Radiation Chemistry*. EDP Sciences; Paris: 2008.

8. Krisch RE, Flick MB, Trumbore CN. *Radiat Res.* 1991; 126:251–259. [PubMed: 1850853]
9. Alpen, EL. *Radiation Biophysics.* PRENTICE-HALL, INC; New Jersey: 1990.
10. O’Neil, P. *Radiation Chemistry: Present Status and Future Trends.* Elsevier Science; Amsterdam: 2001. Radiation-induced damage in DNA.
11. Chatgilliloglu C, O’Neil P. *Exp Gerontol.* 2001; 36:1459–1471. [PubMed: 11525869]
12. Lehnert, S. *Biomolecular Action of Ionizing Radiation.* Taylor & Francis; New York, London: 2008.
13. International Commission on Radiation Units and Measurements. *ICRU Report 31.* ICRU; Washington, DC: 1979.
14. Pimblott SM, La Verne JA. *Radiat Phys Chem.* 2007; 76:1244–1247.
15. Sanche, L. Low-energy electron interaction with DNA. In: Greenberg, MM., editor. *Radical and Radical Ion Reactivity in Nucleic Acid Chemistry.* John Wiley & Sons, Inc; New Jersey: 2009.
16. Sanche L. *Mass Spectrom Rev.* 2002; 21:349–369. [PubMed: 12645089]
17. Sanche L. *Eur Phys J D.* 2005; 35:367–390.
18. Barilla J, Lokajík M. *J Theor Biol.* 2000; 207:405–414. [PubMed: 11082309]
19. Ptasińska S, Sanche L. *Physical Review E.* 2007; 75:031915-1-5.
20. Hall, EJ., Giaccia, AJ. *Radiobiology for the Radiologist.* Lippincott Williams & Wilkins; Philadelphia: 2006.
21. Von Sonntag, C. *Free-Radical-Induced DNA damage and its Repair.* Springer-Verlag; Berlin, Heidelberg: 2006.
22. Morse ML, Dahl RH. *Nature.* 1978; 271:660–662. [PubMed: 342974]
23. Hollaender A, Stapleton GE. *Physiol Rev.* 1953; 33:77–84. [PubMed: 13013833]
24. Skarsgard LD, Harrison I. *Radiat Res.* 1991; 127:243–247. [PubMed: 1886978]
25. Hall EJ. *Int J Radiat Oncol Biol Phys.* 1982; 8:323–325. [PubMed: 7107349]
26. Jamieson D, Chance B, Cadenas E, Bovens A. *Ann Rev Physiol.* 1986; 48:703–719.
27. Hassy-Dow, K., Hilderly, LJ. *Nursing care in Radiation Oncology.* WB Saunders; 1992.
28. Wilkes, GM., Barton-Burke, M. *2005 Oncology Nursing Drug Handbook.* Jones & Bartlett Publishers; 2004.
29. Quintiliani M. *Int J Radiat Biol.* 1986; 50:453–594.
30. Cai Z, Cloutier P, Hunting D, Sanche L. *J Phys Chem B.* 2005; 109:4796–4800. [PubMed: 16851564]
31. Brun É, Cloutier P, Sicard-Roselli C, Fromm M, Sanche L. *J Phys Chem B.* 2009; 113:10008–10013. [PubMed: 19603845]
32. QIAprep® Miniprep Handbook. [www.qiagen.com](http://www.qiagen.com)
33. Sambrook, R. *Molecular Cloning, A Laboratory Manual.* Cold Spring Harbor Laboratory Press; New York: 2001.
34. Cecchini S, Girouard S, Huels MA, Sanche L, Hunting D. *Radiat Res.* 2004; 162:604–615. [PubMed: 15548110]
35. Manchester KL. *Biotechniques.* 1996; 20:968–970. [PubMed: 8780864]
36. Doshi R, Day PJR, Tirelli N. *Biochem Soc Trans.* 2009; 37:466–470. [PubMed: 19290883]
37. Wilfinger WW, Mackey K, Chomczynski P. *Biotechniques.* 1997; 22:474–481. [PubMed: 9067025]
38. Glasel JA. *Biotechniques.* 1995; 18:62–63. [PubMed: 7702855]
39. Adams, RLP., Knowler, T., Leader, DP. *The Biochemistry of the Nucleic Acids.* Chapman & Hall; 1986.
40. Hoshi M, Goodhead DT, Brenner DJ, Bance DA, Chmielewski JJ, Paciotti MA, Bradbur JN. *Phys Med Biol.* 1985; 30:1029. [PubMed: 4070360]
41. Cai Z, Pan X, Hunting D, Cloutier P, Lemay R, Sanche L. *Phys Med Biol.* 2003; 48:4111–4124. [PubMed: 14727755]
42. Rye HS, Yue S, Quesada MA, Haugland RP, Mathies RA, Glazer AN. *Methods Enzymol.* 1992; 217:414–431.

43. <http://rsb.info.nih.gov/ij/>.
44. National Institute of Standards & Technology. NIST. <http://physics.nist.gov/PhysRefData/XrayMassCoef/>
45. Huels MA, Boudaïffa B, Cloutier P, Hunting D, Sanche L. J Am Chem Soc. 2003; 125:4467–4477. [PubMed: 12683817]
46. Dumont A, Zheng Y, Hunting D, Sanche L. J Chem Phys. 2010; 132:045102-1-8. [PubMed: 20113068]
47. Henke BL, Smith JA. J Appl Phys. 1977; 48:1852–1866.
48. Jaeckel R, Wagner B. Vacuum. 1963; 13:509–511.
49. Hopkins J, Riviere JC. Brit J Phys. 1964; 15:941–946.
50. LaVerne JA, Pimblott SM. Radiat Res. 1995; 141:208–215. [PubMed: 7838960]
51. Pimblott SM, Siebbeles LD. Nucl Instrum Methods Phys Res B. 2002; 194:237–250.
52. Martin F, Burrow PD, Cai Z, Cloutier P, Hunting D, Sanche L. Phys Rev Lett. 2004; 93:068101-1-4. [PubMed: 15323664]
53. Folkard M, Prise KM, Vojnovic B, Brocklehurst B, Michael BD. Int J Radiat Biol. 2000; 76:763–771. [PubMed: 10902730]
54. Panajotovic R, Martin F, Cloutier P, Hunting D, Sanche L. Radiat Res. 2006; 165:452–459. [PubMed: 16579658]
55. Metcalfe, PP., Kron, T., Hoban, P. The Physics of Radiotherapy X-Rays and Electrons. Medical Physics Publishing; 2007.
56. Zaviropulo N, Chipev FF, Shpenik OB. Technical Physics. 2005; 50:402–407.
57. Kaila, K. The 12th EISCAT international Workshop; Sweden: Incoherent Scatter Radar School; 2005.
58. Tóth I, Campeanu RI, Chi V, Nagy L. Eur Phys J D. 2008; 48:351–354.
59. Illenberger, E. Gaseous Molecular Ions, An Introduction to Elementary Processes Induced by Ionization. Steinkopf Verlag, Darmstadt and Springer Verlag; New York: 1992.
60. Massey, HSW. Negative Ions. Cambridge University Press; London: 1976.
61. Spence D, Burrow PD. J Phys B: Atom Molec Phys. 1979; 12:179–184.
62. Eliasson B, Kogelschatz U. J Phys B: At Mol Phys. 1986; 19:1241–1247.
63. Huels MA, Parenteau L, Michaud M, Sanche L. Physical Review A. 1995; 51:337–349.
64. Galuska D, Manole D, Vladiu R, Matejcek S, Skalny JD. Journal of Optoelectronics and Advanced Materials. 2005; 7:2371–2378.
65. Misiaszek R, Crean C, Joffe A, Geacintov NE, Shafirovich V. J Biol Chem. 2004; 279:32106–32115. [PubMed: 15152004]
66. Schulz GJ. Reviews of Modern Physics. 1973; 45:423–486.
67. Allan M. J Phys B: At Mol Opt Phys. 1995; 28:5163–5175.
68. Ptasińska S, Denifl S, Grill V, Märk TD, Illenberger E, Scheier P. Phys Rev Lett. 2005; 95:093201-1-4. [PubMed: 16197213]
69. Ptasińska S, Denifl S, Scheier P, Märk TD. J Chem Phys. 2004; 120:8505–8511. [PubMed: 15267776]
70. Denifl S, Ptasińska S, Probst M, Hrušák J, Scheier P, Märk TD. J Phys Chem A. 2004; 108:6562–6569.
71. Wiseman H, Halliwell B. Biochem J. 1996; 313:17–29. [PubMed: 8546679]
72. Dedon PC, Tannenbaum SR. Archives of Biochemistry and Biophysics. 2004; 423:12–22. [PubMed: 14989259]
73. Halliwell B. Mutation Research. 1999; 443:37–52. [PubMed: 10415430]
74. Bertout JA, Patel SA, Celeste M. Nature Reviews Cancer. 2008; 8:967–975. [PubMed: 18987634]
75. Breen AP, Murphy JA. Free Radic Biol Med. 1995; 18:1033–1077. [PubMed: 7628729]
76. Aruoma OI, Halliwell B, Dizdaroglu M. J Biol Chem. 1989; 264:13024–13028. [PubMed: 2546943]
77. Halliwell B, Aruoma OI. FEBS Letters. 1991; 281:9–19. references therein. [PubMed: 1849843]

78. Tofigh S, Frenkel K. *Free Radic Biol Med.* 1989; 7:131–143. [PubMed: 2509298]



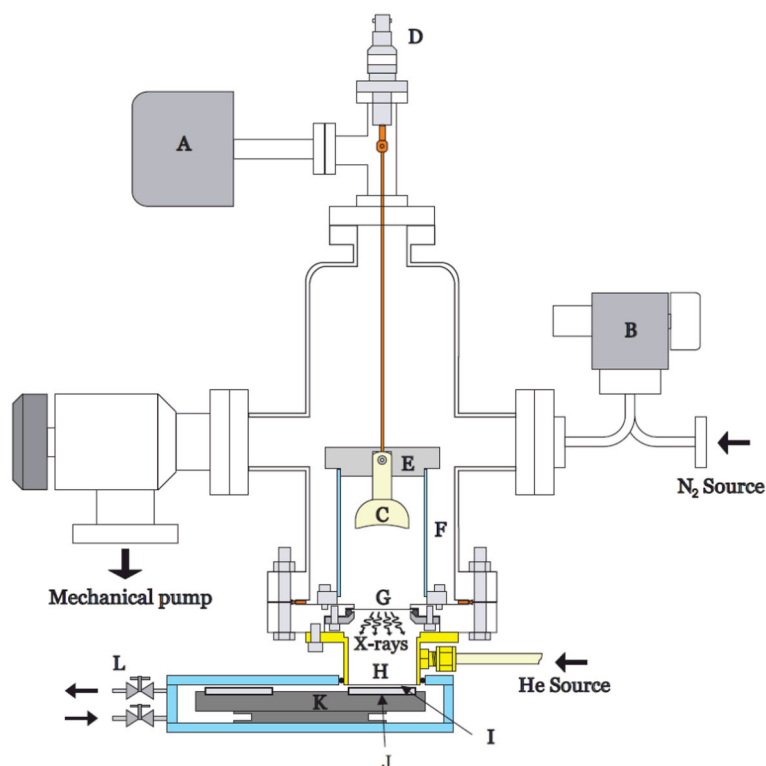


**Figure 1.** Schematic view of the apparatus used to irradiate DNA samples with 1.5 keV Al K $\alpha$  X-ray photons under nitrogen and oxygen gas at atmospheric pressure: (A) baratron, (B) adjustable leak valve, (C) concave aluminum cathode, (D) high voltage electric feedthrough, (E) glass-ceramic (Macor) support, (F) quartz tube, (G) aluminum foil target, (H) He-filled enclosed volume, (I) thin foil of Mylar, (J) aluminum plate as sample holder, (K) rotating disk, and (L) gas circulation valves.

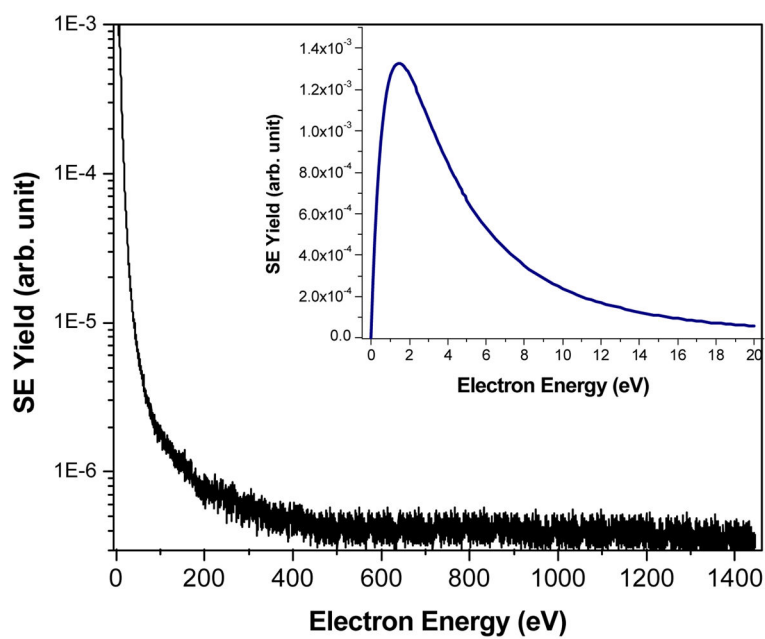


**Figure 2.** Energy spectra of Al K<sub>α</sub> X-ray induced secondary electron emission from a tantalum substrate in two different energy ranges.

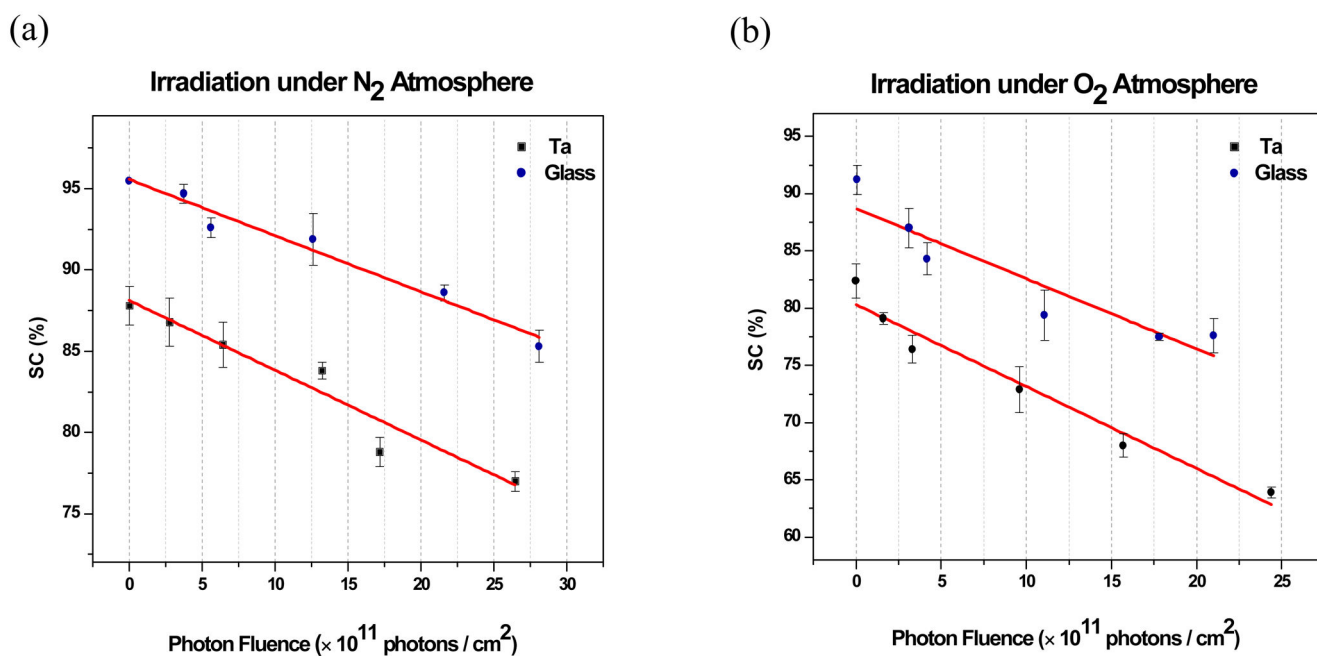


**Figure 3.**

Exposure-response curves for the loss of the supercoiled DNA deposited on glass and tantalum substrates and irradiated by 1.5 keV X-rays under (a) N<sub>2</sub> and (b) O<sub>2</sub> atmospheres. The points represent the means of three yield measurements and the error bars represent the standard deviation of the means.

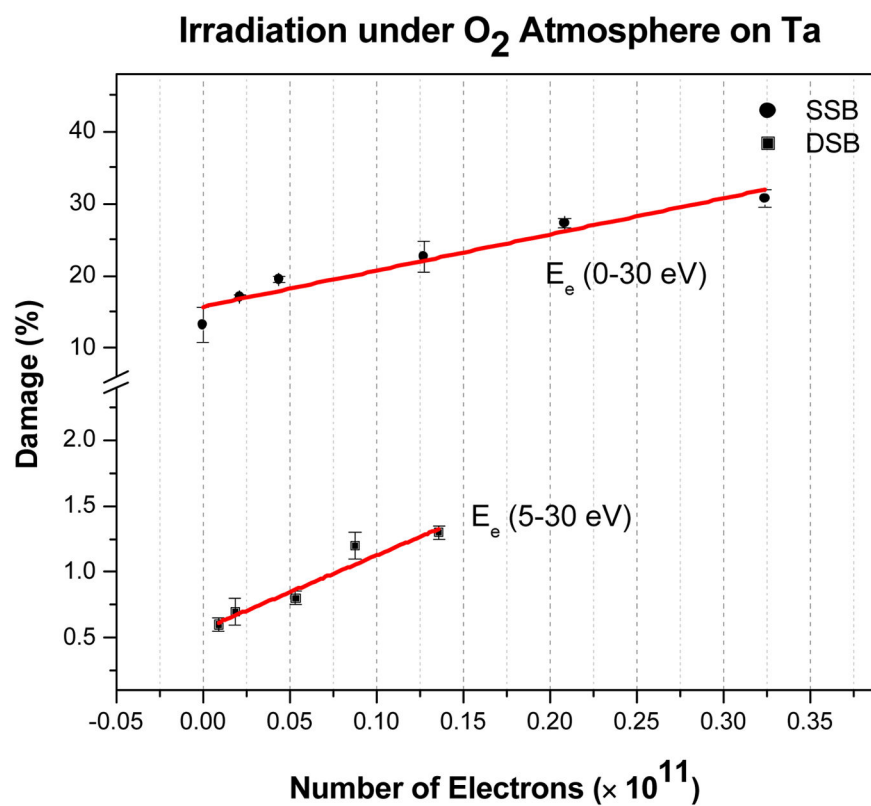


**Figure 4.** Exposure-response curves for formation of circular (SSB) and linear DNA (DSB) in an O<sub>2</sub> environment from LEE interaction with plasmid DNA deposited on tantalum substrates. The points represent the means of three measurements and the error bars represent standard deviation of the means.

Percentage yields of undamaged DNA as well as induced damage in un-irradiated SML films of the plasmid deposited on tantalum and glass substrates under N<sub>2</sub> and O<sub>2</sub> atmospheres.

**Table 1**

Plasmid Conformation	Fresh Plasmid DNA in Solution	Lyophilized and Recovered DNA (Ta & Glass)	N <sub>2</sub>		O <sub>2</sub>	
			Tantalum	Glass	Tantalum	Glass
SC (%)	96 ± 1	95 ± 1	87.8 ± 1.2	94.7 ± 0.6	82.4 ± 1.5	91.2 ± 1.3
SSB (%)	2 ± 1	3 ± 1	11 ± 1.8	2.5 ± 0.5	13.2 ± 2.4	6.9 ± 1.4

**Table 2**

Percentage yield per  $10^{12}$  photons.cm<sup>-2</sup> for the loss of supercoiled DNA in 5ML films of the plasmid deposited on tantalum and glass substrates under N<sub>2</sub> and O<sub>2</sub> gas at atmospheric pressure. The enhancement factor (EF) in each atmosphere is calculated by dividing the slope of the exposure-response curve obtained with DNA on tantalum by that obtained with DNA deposited on glass. The yield of LEE-induced damage per  $10^{14}$  DNA molecule<sup>-1</sup>.electron<sup>-1</sup> in the 5ML films is shown in the last column.

<b>Substrate Environment</b>	<b>Tantalum</b>	<b>Glass</b>	<b>Enhancement Factor (EF)</b>	<b>Yield of LEE damage</b>
N <sub>2</sub>	4.9 ± 0.7	3.6 ± 0.6	1.4	96
O <sub>2</sub>	9.0 ± 0.8	6.8 ± 0.9	1.3	175
O <sub>2</sub> / N <sub>2</sub>	1.8	1.9		

**Table 3**

The  $G$  values for soft X-rays and LEEs under  $N_2$  and  $O_2$  conditions (in D / 100eV and nmol / J).

Damage	$G_X$		$G_{LEE}$		$G_{LEE} / G_X$
	D / 100eV	nmol / J	D / 100eV	nmol / J	
$N_2$	$0.63 \pm 0.06$	$65 \pm 6$	$2.19 \pm 0.15$	$227 \pm 15$	3.5
$O_2$	$1.20 \pm 0.09$	$124 \pm 9$	$4.0 \pm 0.15$	$415 \pm 15$	3.4
$O_2 / N_2$		1.9		1.8	